Application Note

Cell Biology, Biochemical Assays, Enzymology

Monitoring of Protein Kinase Activity using Next Generation CSox-based Substrate Sensors

Peter J. Brescia, Jr., and Peter Banks, BioTek Instruments, Inc., Winooski, VT USA
Susan Cornell-Kennon and Erik Schaefer, AssayQuant Technologies, Inc., Marlboro, MA USA
Barbara Imperiali, Massachusetts Institute of Technology (MIT), Cambridge, MA USA

Key Words:

CSox

Kinase

CHEF

PhosphoSens

ERK1/2

MAPK

EGFR RTK

BioTek Instruments, Inc.
P.O. Box 998, Highland Park,
Winooski, Vermont 05404-0998 USA
Phone: 888-451-5171
Outside the USA: 802-655-4740
Email: **customercare@biotek.com**
www.biotek.com
Copyright © 2017

Abstract

There are greater than 500 protein kinases, many of which have been shown to be dysregulated in disease states and comprise greater than 30% of all drug development. Harnessing chelation-enhanced fluorescence (CHEF) with the sulfonamido-oxine (Sox) chromophore in peptide or protein substrates has created a simple yet powerful method to measure the activity of protein kinases using a direct, homogeneous and continuous (kinetic) format. This kinetic assay platform allows elucidation of drug mechanism of action and is increasingly being applied earlier in the drug development process to address challenges and opportunities for next generation kinase inhibitors.

Introduction

Protein kinases and phosphatases are ubiquitous in nature and are critical enzymes that regulate the complexity of signal transduction pathways in normal and disease states. A major focus of all research efforts is addressing drug development for these enzymes that spans many disease areas[1-3]. Kinases form a class of signaling enzymes that carry out the transfer of a phosphate group from ATP to a serine, threonine or tyrosine residue with the target protein, which can dramatically change the activity, location within a cell, and the nature of the signaling complexes formed with that protein. The protein phosphatases catalyze the removal of the phosphate from the target protein, thereby creating a dynamic balance. Both enzyme classes regulate diverse cellular functions including cell growth, differentiation, metabolism, proliferation and survival. Abnormal signaling in any one of these pathways can have severe consequences resulting in a diseased state.

The ability to accurately and precisely quantify kinase activity and define the effects of compounds that modulate this activity is essential for understanding the complex biology of phosphoregulation and for the development and monitoring of effective therapeutic agents against these enzymes[4-8]. Precise activity measurements are also critical for understanding the effects of mutations on enzyme function in determining signal transduction and cellular fate decisions[9,10].

A kinetic kinase assay platform has been developed by AssayQuant Technologies, Inc. that provides a simple, one-step homogeneous, fluorescence-based assay for rapid, sensitive and continuous detection of serine/threonine and tyrosine kinase activities. The assay directly measures the catalytic activity of target kinases using optimized peptide substrates under optimal conditions including pH, selected metal ion cofactors, and low to physiological (mM) ATP concentrations allowing both ATP-competitive and ATP non-competitive (allosteric) kinase inhibitors to be selected and characterized. Here we demonstrate utility across a variety of applications. Although this article focuses on measuring protein kinase activity, the platform also allows study of protein phosphatases using the appropriate phosphopeptide substrates[11,12].

Assay Principle

The Chelation-Enhanced Fluorescence (ChEF) method for protein kinase sensing was invented by the Imperiali laboratory at the Massachusetts Institute of Technology (MIT) and has been extensively validated[13-16]. The ChEF sensing mechanism exploits a synthetic α-amino acid with a side chain bearing an 8-hydroxyquinoline derivative (sulfonamido-oxine, Sox), which upon coordination to Mg(II), relays information on the phosphorylation state of proximal serine,

threonine or tyrosine residues in peptide- and protein-based kinase substrates (Figure 1). In the absence of phosphorylation, Sox shows low affinity for Mg(II); upon phosphorylation, Mg(II) affinity is enhanced due to the advantageous chelate effect, involving the Sox and the introduced phosphate group, and fluorescence is turned on. Since it was first introduced, the Imperiali laboratory has continually improved the technology for the ChEF method[13-21]. AssayQuant Technologies, Inc., who holds the exclusive license for the technology, has been systematically integrating improvements from MIT and through in house innovation to deliver optimum performance of their PhosphoSens® product line, which currently includes 167 validated protein kinases and 27 Sox-based substrates (www.assayquant.com). Assays can be performed in continuous kinetic mode, using commonly available fluorescence plate readers in 96-, 384- and 1536-well plate formats and a wide range of sample types including recombinant enzymes, immunoprecipitated kinases, and crude cell or tissue lysates[13-23]. The platform is ideal for understanding mechanism of action, but is increasingly being applied earlier in the drug development process to define and optimize next generation kinase inhibitors by enabling precise determinations of kinase activity regulation, kinase inhibitor screening, structure-activity relationships (SAR), and inhibitor parameter determinations (IC_{50}, K_i, k_{inact}, residence time, mechanism of action)[24-27].

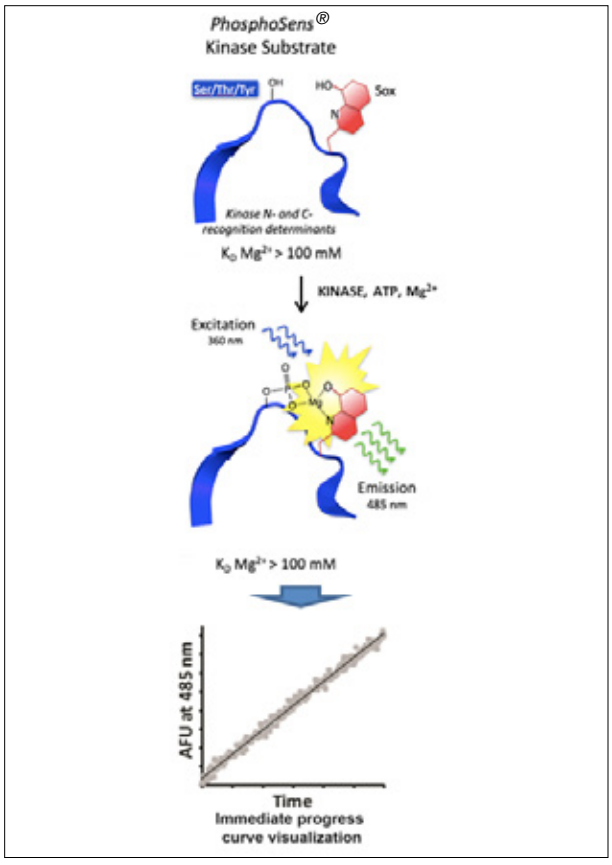

Figure 1. **Chelation Enhanced Fluorescence (ChEF) Mechanism for Direct Protein Kinase Activity Sensing.** The fluorescence properties of the Mg(II) coordinated Sox are: λ_{ExMax} 360 nm and λ_{EmMax} 485 nm.

Figure 2A illustrates typical fluorescence changes upon phosphorylation of a peptide substrate and Figure 2B shows excitation and emission spectra of a typical phosphorylated peptide. The λ_{ExMax} of the chelated Mg(II) with the 8-hydroxyquinoline is 360 nm and the λ_{EmMax} is 485 nm. Since the fluorescence emission spectrum is relatively broad (see Figure 2B), fluorescence emission can be monitored between 475-505 nm with minimal loss of signal intensity. Efforts to extend the emission to >600 nm are in progress.

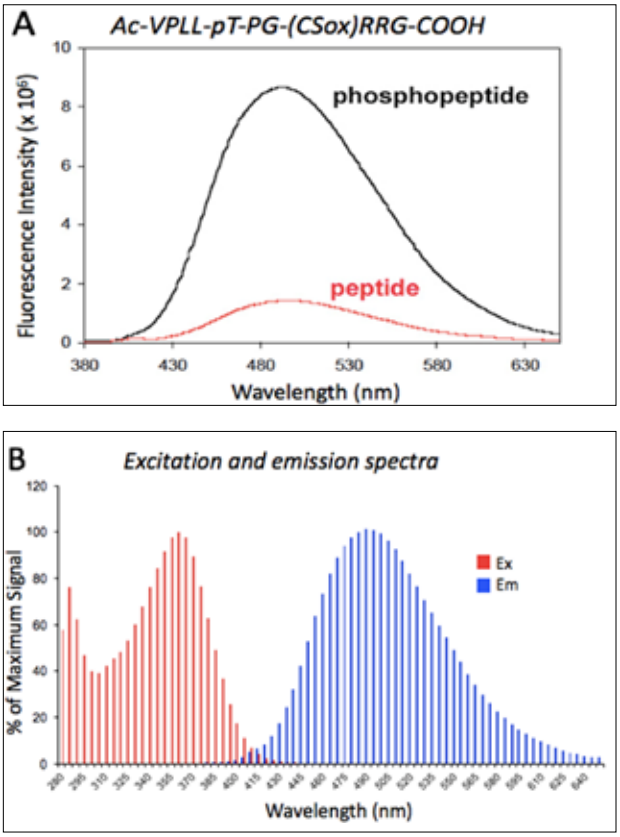

Figure 2. **Fluorescence Spectra of PhosphoSens® Peptides. (A)** Typical fluorescence changes upon phosphorylation of a peptide substrate for ERK1/2 MAPK: Ac-VPLL-pT-PG-[CSox]-RRG-COOH. **(B)** Excitation and Emission spectra. The λ_{ExMax} of chelated Mg(II) with the 8-hydroxyquinoline is 360 nm and the λ_{EmMax} is 485 nm.

Materials and Methods

Materials

Materials were sourced and prepared as per the manufacturers' recommendations. All kinases were from Carna Biosciences (www.carnabio.com). Briefly, the assay reaction was initiated by the addition of a master mix containing either a protein kinase or the CSox-peptide substrate to a well containing the final component needed to start the reaction. Typical final concentrations of each reaction component are as follows: 50 mM HEPES, pH 7.5, 1 mM ATP (or adjusted as needed), 1 mM DTT, 0.01% Brij-35, 0.5 mM EGTA, 10 mM $MgCl_2$, 10 µM peptide substrate, 0.1-10 nM kinase (or adjusted as needed), Additional co-factors or additives (as needed).

The peptide substrate was resuspended to create a 1 mM (100x) stock. For both peptide and ATP, a 10x working solution was prepared as necessary in ultrapure H_2O just before use. DTT working solution, 10x, was prepared from 1000x stock in ultrapure H_2O just before use. Kinase reaction master mix was prepared as per manufacturers' instructions. Kinases were prepared as a 5x working concentration just before use in kinase dilution buffer and added to the wells to initiate reactions. Fluorescent measurements were taken at 30 °C either kinetically or as an end point measurement.

Kinase titrations were prepared as an 11-point, 2-fold serial dilution using 1x kinase dilution buffer as well as a no-kinase control. Each dilution in the series represented 5x the final concentration of kinase in the reaction resulting in a concentration range that spans 3 log units (e.g., from 20 nM to 20 pM). Samples and standards were plated in triplicate. All assays were performed in Corning half-area, 96-well, white NBS plates (P/N 3824).

Instrumentation

A Synergy™ Neo2 (BioTek Instruments, Inc., Winooski, VT) was used for reading fluorescence intensity in kinetic mode with an excitation wavelength (λ_{ex}) of 360 nm and an emission wavelength (λ_{em}) of 485 nm. Readings were typically performed every 30 seconds for 60 minutes or every 2-3 minutes for 150 minutes.

Data reduction

The background fluorescence was subtracted for each time point from the total fluorescence signal to obtain corrected relative fluorescence units (RFU) values. The corrected RFUs vs. time was plotted. The slope of the initial linear portion of each curve was determined, which is the initial reaction rate (RFU/min., or converted to RFU/pmole kinase/min.). Reaction rates from linear or non-linear (kinases that exhibit a lag phase) fit of the data were generated using Gen5™ software (BioTek Instruments, Inc., Winooski, VT) or by exporting data to GraphPad Prism (La Jolla, CA).

Background: Kinase Kinetic Parameter Analysis

To determine K_m, a fixed concentration of kinase was combined with a serial dilution of a CSox-based peptide substrate. K_m determinations require a range of substrate concentrations, ideally from 0.1- to 2 to 10-fold of the estimated K_m. V_{max} values in $\mu mol.mg^{-1}min^{-1}$ were determined as described below and presented in detail in Lukovic et al.[16].

To determine V_{max}, from the initial rates of product formation, a correction for the decrease in fluorescence intensity due to the substrate consumption was required. The fluorescence intensity at any given time in the reaction is determined from the following equation:

(1)

$$I(t) = f_s S(t) + f_p P(t)$$

where I(t) is the fluorescence intensity, S(t) is the amount of substrate in µM, P(t) is the amount of product in µM, f_s is the fluorescence intensity per µM of substrate, and f_p is fluorescence intensity per µM of product.

The amount of substrate and product at any given point are related by:

(2)

$$S(t) + P(t) = S_0$$

where S_0 is the initial amount of substrate.

Substitution of eq. (2) into eq. (1) followed by rearrangement yields:

(3)

$$P(t) = \frac{I(t) - f_s S_0}{f_p - f_s}$$

The initial velocity of the reaction is the change in the amount of product over time, so taking the derivative of eq. (3) with respect to time gives:

(4)

$$v = \frac{dP(t)}{dt} = \frac{\frac{dI(t)}{dt}}{f_p - f_s}$$

The initial slope of the reaction, dI(t)/dt, should be measured within the first 10% of substrate turnover to ensure initial rate analysis. The constants f_P and f_S were calculated from the standard curves of RFU versus concentration of P and S, respectively. These values will depend on the concentration of Mg^{2+} and the Mg^{2+} dissociation constant of each peptide and were determined empirically under the desired assay conditions. The K_m and V_{max} were determined from a direct, non-linear fit of v vs. [S] plots using the Michaelis-Menten equation:

(5)

$$v = \frac{V_{max}[S]}{K_m + [S]}$$

These determinations are routinely performed using Graphpad Prism Software.

The phosphopeptide standard curve based on enzymatic synthesis of the product was generated by combining a fixed concentration of kinase with a serial dilution of CSox peptide substrate at the same concentrations used in the kinetic assay. Typically, the amount of kinase used to generate the phosphopeptide standard curve is higher than the concentration used in the kinetic analysis in order to ensure complete phosphorylation of the peptide substrate. The kinase concentration required to reach signal saturation will vary between kinases. A titration of kinase was performed, as previously described, with the highest concentration of peptide substrate to determine the amount of kinase required to achieve complete phosphorylation.

Results

CSox-based Substrate Optimization for EGFR RTK

The Epidermal Growth Factor Receptor (EGFR) is a Receptor Tyrosine Kinase (RTK) that has been intensely studied to understand its complex biology, the generation of kinase inhibitors, the appearance of mutations that confer drug resistance and to define the best sequence of treatments for human cancer[24,26-29]. To develop improved Sox-based assays for the EGFR, partially degenerate peptide libraries, incorporating the Sox chromophore, were used to screen for sensors with increased reaction rates. Reactions conditions were optimized and two rounds of selection were performed.

Reactions were incubated at 30 °C for 120 minutes and fluorescent intensity data were collected every 5 minutes and plotted as relative fluorescent units corrected for background (RFU, corrected) versus time (Figure 3). Background subtraction was achieved by subtracting RFU values from a no kinase control at each time point with the same peptide concentration from each kinase reaction. Corrected RFU values were plotted versus time for determination of the initial reaction velocities (slope of the line; RFU/min.) from the linear portion of each curve. Each line in the graph represents a different sequence consisting of either a single amino acid substitution (Round 1) or combinations of favorable substitutions (Round 2) as identified in Round 1.

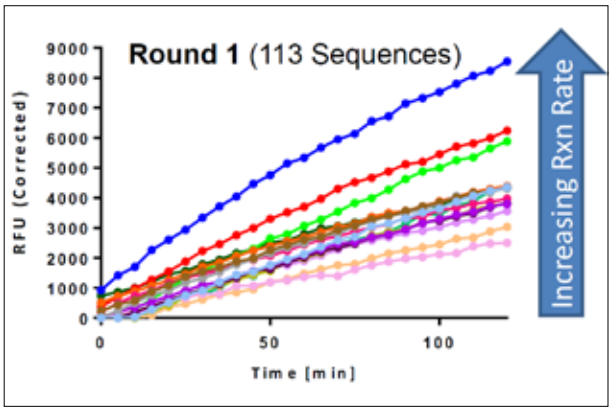

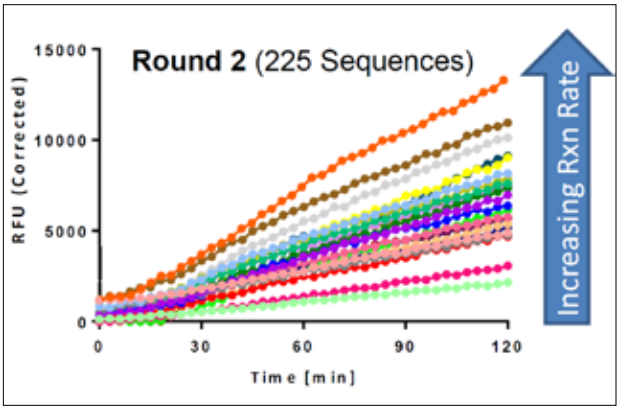

Figure 3. **Optimization of degenerate peptide sequences.** Two rounds of selection were performed with partially degenerate Sox-peptide libraries. The steeper the curve, the higher the reaction rate.

This approach allowed the selection of optimum Sox-based sequences for measurement of wild-type EGFR and each of the clinically-relevant mutants (Figure 4). These data demonstrate the dramatic increase in kinase activity observed with each of these clinically-relevant mutants, which drives tumor growth and metastasis and resistance to first-line drugs.

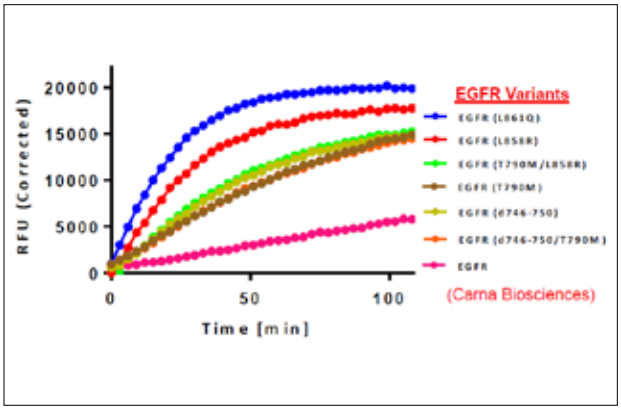

Figure 4. **Progress curves generated using the PhosphoSens® AQT0099 Sox-based substrate incubated with 5 nM of the wild-type EGFR and each of the clinical variants.**

Enzyme Titration

Kinase titration reactions were performed with selected peptide substrates to determine linearity. Reactions were incubated at 30 °C for 150 minutes and fluorescent intensity data were collected every 3 minutes and plotted versus time. Each line represents a different enzyme concentration (Figure 5a and 5c). Initial velocity determinations were calculated for each reaction and plotted versus each enzyme concentration. The data demonstrate linearity across a range of kinase concentrations from 10 nM down to 160 pM for the wild-type EGFR and from 1.3 nM down to 39 pM for the EGFR (T790M/L858R) (Figure 5b and 5d), highlighting the dramatic increase in activity of this mutant variant. Any kinase concentration that provided a linear signal with time and resulted in <10% of the substrate being phosphorylated were used for subsequent experiments.

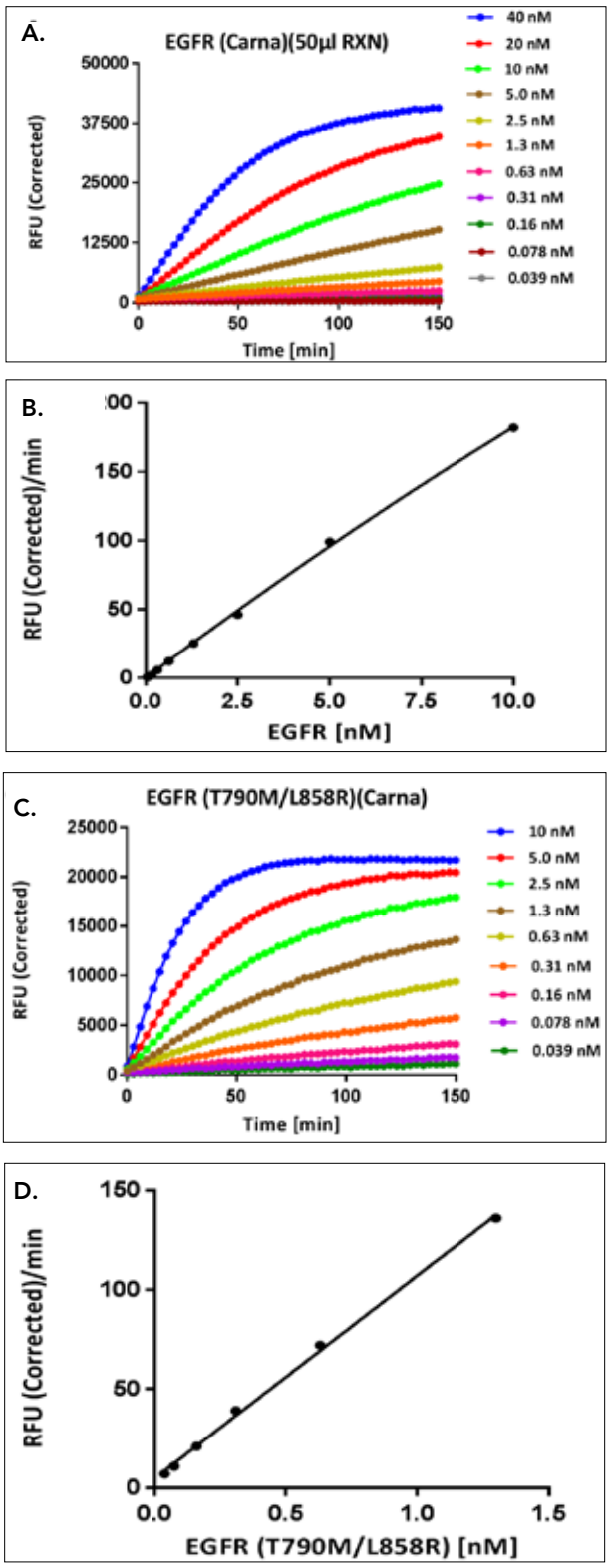

Figure 5. Representative data from a kinase-titration experiment. (**A**) EGFR WT tyrosine kinase with the PhosphoSens® AQT0099 peptide substrate, (**B**) Linearity across a range of EGFR WT concentrations, (**C**) EGFR(T790M/L858R) tyrosine kinase with the PhosphoSens® AQT0099 peptide substrate, and (**D**) Linearity across a range of EGFR(T790M/L858R) concentrations.

Z' with Different [Enzyme] and Reaction Volumes

Assay performance was examined to determine the impact of varying the final reaction volume (25, 50 and 75 µL) and EGFR concentration (0.25 to 1.25 nM) on precision determined by calculation of Z' values (Figure 6, Table 1). A final reaction volume of 50 µL is recommended by the manufacturer, however, the final choice is based on assay requirements (i.e., enzyme and substrate concentration, nature of inhibitor studies, etc.).

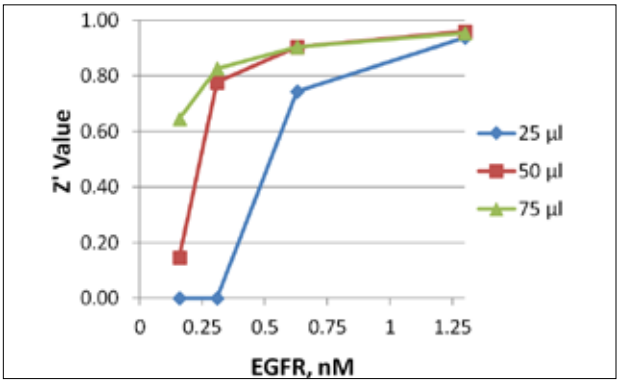

Figure 6. Effect of assay volume on precision with Z' values plotted against EGFR concentration for each assay volume.

Conc (nM)	25 µl	50 µl	75 µl
0.039	N/A	N/A	N/A
0.078	N/A	N/A	0.47
0.16	N/A	0.15	0.65
0.31	N/A	**0.78**	**0.83**
0.63	0.74	0.90	0.90
1.3	**0.94**	0.96	0.95
2.5	0.97	0.97	0.98
5	0.97	0.98	0.98
10	0.97	0.98	0.97
20	0.96	0.98	0.96
40	0.97	0.96	0.98

Table 1. Z' Values for Different Final Reaction Volumes and EGFR Concentrations. Bolded Z' values correspond to the Lower Limit of Quantitation (LLOQ), which is the lowest concentration of enzyme where the CV is still <20%.

Assay formats with Z' values >0.5 are considered to be robust. The PhosphoSens® assay format typically delivers Z' values >0.7, even at very low enzyme concentrations, highlighting the very high precision of the Sox-based assay platform.

Substrate Titration for K_m and V_{max} Determination

The reaction velocities for each substrate concentration were then determined by incubating a 1.5-fold serial dilution of peptide substrate, 200 to 2.3 µM, with a constant concentration of each EGFR. Each dilution series was analyzed in triplicate as described above (Figures 7 and 8).

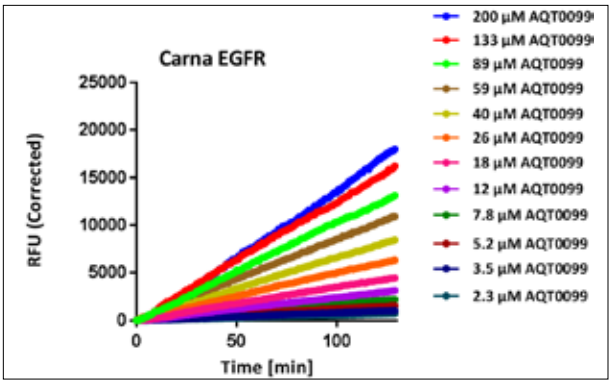

Figure 7. **Representative data from a titration of the PhosphoSens® Peptide Substrate AQT0099.** Serially diluted substrate was incubated with 8 nM EGFR for 120 minutes at 30 °C to determine reaction velocities (RFU Corrected/min) at each substrate concentration.

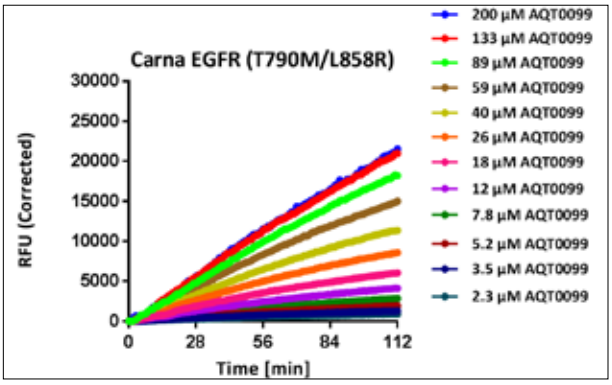

Figure 8. Serially diluted PhosphoSens® Peptide Substrate AQT0099 was incubated with 1 nM EGFR (T790M/L868R) for 112 minutes at 30 °C to determine reaction velocities (RFU Corrected/min) at each substrate concentration.

Conversion of Rates from RFU to µM/min

Generation of a phosphopeptide standard curve was performed as described for Figure 8, but using 20-fold higher levels of the EGFR (T790M/L858R) in the reaction to ensure that all of the PhosphoSens® Peptide Substrate AQT0099 was converted to its phosphorylated form (Figure 9). The standard curves were constructed by plotting the saturating RFU values for each sample versus the concentration of the peptide substrate in the reaction (Figure 10). The slope of the standard curve was determined and used to convert reaction rate velocities. Velocities were converted to µM/min by dividing the reaction velocities (RFU/min) by the slope of the phosphopeptide standard curve (RFU/µM) (Table 2). The converted velocities were plotted versus the substrate concentration and the data fit to the Michaelis-Menten equation for determination of K_m and V_{max} (Figure 11a and 11b). For EGFR the K_m and V_{max} were determined to be 79 ±1.9 µM and 0.32 ±0.0037 µM/min, respectively. For the EGFR (T790M/L858R), the K_m and V_{max} were determined to be 92 ±5.0 µM and V_{max} equal to 0.55 ±0.017 µM/min, respectively. Since the amount of substrate being used (10 µM) is much less than the K_m, the difference in K_m are less significant, however the fact that the V_{max} for the EGFR (T790M/L858R) mutant under these conditions is 1.7-fold greater is dramatic and contributes to the cancer phenotype.

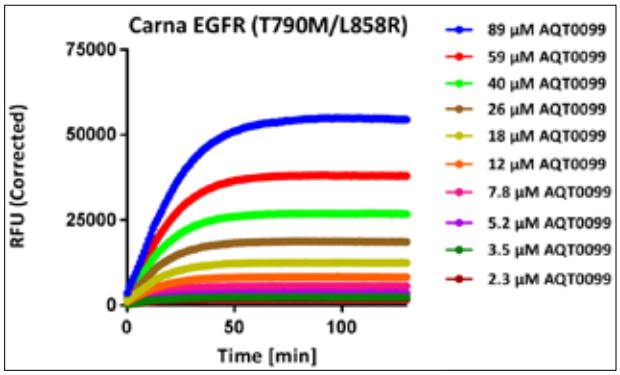

Figure 9. Phosphopeptide standard curve: 20 nM EGFR (T790M/L858R) was used to completely phosphorylate all of the PhosphoSens® Peptide Substrate AQT0099 at each concentration to determine the saturating RFU values for each sample and to then generate a phosphopeptide standard curve.

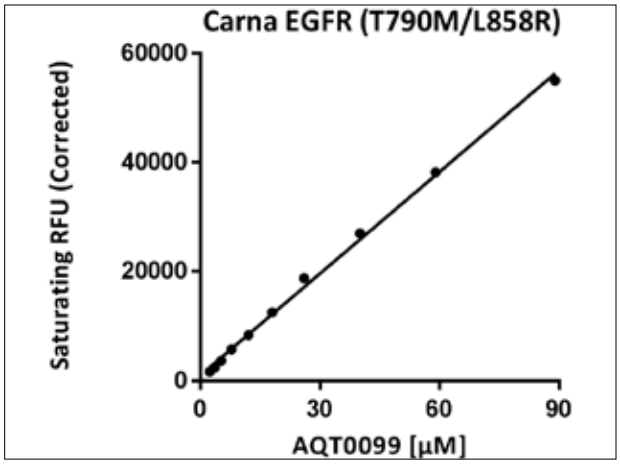

Figure 10. The slope for this curve was determined to be 621 ±11 RFU Corrected/µM, which is used to convert reaction velocities from RFU/min to µM/min.

Conc (µM)	EGFR Reaction Velocity (µM/min)	EGFR (T790M/L858R) Reaction Velocity (µM/min)
2.3	0.0093	0.0120
3.5	0.013	0.018
5.2	0.019	0.026
7.8	0.029	0.040
12	0.040	0.058
18	0.058	0.085
26	0.082	0.120
40	0.11	0.17
59	0.14	0.22
89	0.17	0.27
133	0.20	0.32
200	0.23	ND

Table 2. Reaction Velocities (µM/min) were determined by dividing the reaction velocities from the kinetic progress curves (RFU Corrected/min) by the slope from the phosphopeptide standard curve (621 ± 11 RFU Corrected/µM).

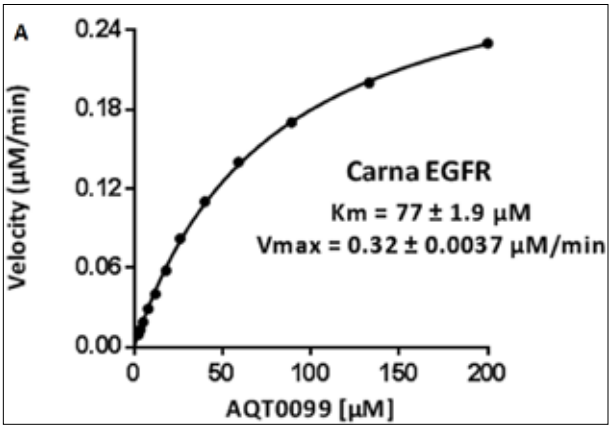

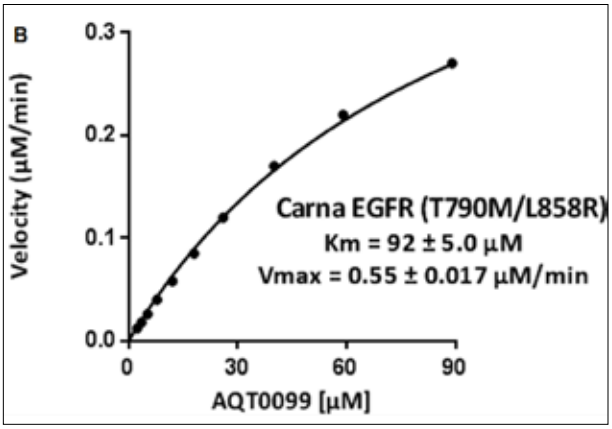

Figure 11. Data was fit with the Michaelis-Menten equation to determine the K_m and V_{max} for the EGFR and EGFR (T790M/L858R). (A) EGFR and (B) EGFR (T790M/L858R).

Inhibitor Characterization

Progress curves were generated using 3 nM EGFR or 1 nM EGFR (T790M/L858R) with 20 µM of PhosphoSens® Peptide Substrate AQT0099 in the absence (untreated control) or presence of the tyrosine kinase inhibitor Tarceva (0 - 5 µM) for 150 minutes at 30 °C. The resulting RFU signals over time were corrected by subtracting background fluorescence determined in control (no kinase) reactions and initial reaction velocities determined as described above (Figure 12).

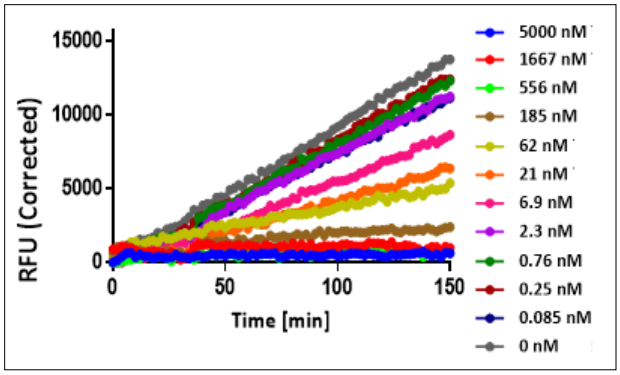

Figure 12. Progress curves generated with each concentration of Tarceva (0 - 5 µM).

The resulting reaction rates (RFU/min.) values were normalized as a percentage of the untreated (no inhibitor) controls and plotted versus the Tarceva concentration (Figure 13) and the IC_{50} values were determined using a 4-parameter logistic curve fit. Note that each data point is the mean ±std dev. and the error bars aren't visible due to the high precision of the PhosphoSens® assay format.

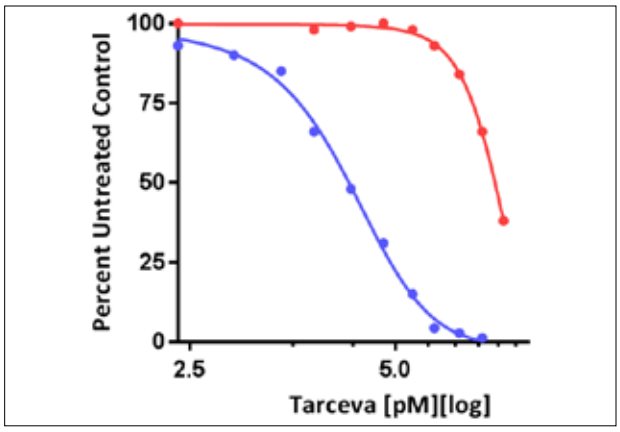

Figure 13. Inhibition curves for EGRF and EGFR (T790M/L858R) in response to the potent tyrosine kinase inhibitor Tarceva.

For the EGFR, the IC_{50} value was determined to be 20 ±0.29 nM, which is similar to the IC_{50} value of 40 nM reported by Kitagawa, et al. (2012)[30], determined under similar conditions with 1 mM ATP. The IC_{50} value determined for the EGFR (T790M/L858R) was 7.6 ±0.19 µM or 380-fold less sensitive to Tarceva, illustrating the resistance to drug that develops in patients.

Conclusion

The enabling features and benefits of the PhosphoSens® detection technology and the Synergy™ Neo2 HTS Multi-Mode Microplate Reader from Biotek Instruments, delivers a powerful combination with improved performance for drug discovery efforts for next generation protein kinase inhibitors. The platform delivers continuous (kinetic) and highly precise measurements of protein kinase (and phosphatase) activity in an easy to use, one-step homogeneous format that increases the quality of information and improves throughout, while reducing hands-on time. AssayQuant has validated 167 protein kinase target assays and 27 PhosphoSens® substrates, including both highly-generic and highly-selective sensors. The use of generic sensors allows screening of a large number of recombinant kinases with maximum flexibility, while highly-selective sensors enable quantitative kinase profiling in crude (unfractionated) cell and tissue lysates. The PhosphoSens® platform is ideal for studying inhibitor mechanism of action and potency, enzyme activation or profiling with a wide range of samples, including purified enzymes and crude cell or tissue lysates, to meet the diverse needs of modern drug discovery.

References

1. Nematullah M1, Hoda MN2, Khan F3. Protein Phosphatase 2A: a Double-Faced Phosphatase of Cellular System and Its Role in Neurodegenerative Disorders. Mol Neurobiol. **2017**, 10.1007/s12035-017-0444-3.

2. Chang AN1, Kamm KE2, Stull JT2. Role of myosin light chain phosphatase in cardiac physiology and pathophysiology. J Mol Cell Cardiol. **2016**, 101:35-43.

3. Matsui WH1. Cancer stem cell signaling pathways. Medicine (Baltimore). **2016** (1 Suppl 1):S8-S19.

4. Fabbro, D., 25 Years of Small Molecular Weight Kinase Inhibitors: Potentials and Limitations, Mol Pharmacol **2015**, 87, 766-775.

5. Roskoski, R., Jr., A historical overview of protein kinases and their targeted small molecule inhibitors, Pharmacol Res **2015**, 100, 1-23.

6. Beck, Jon R.; Peterson, Laura B.; Imperiali, Barbara; Stains, Cliff I. Quantification of protein kinase enzymatic activity in unfractionated cell lysates using CSox-based sensors. Curr Prots in Chem Biol. **2014**; 6 (3), 135–156.

7. Gough, N. R., Focus Issue: Tracking Reproducibility and Accuracy in Cell Signaling Experiments, ScienceSignaling **2015**, 8, eg4.

8. Janes, K. A., An analysis of critical factors for quantitative immunoblotting, Sci Signal **2015**, 8, rs2.

9. Mondal, J.; Tiwary, P.; Berne, B. J., How a Kinase Inhibitor Withstands Gatekeeper Residue Mutations, Journal of the American Chemical Society **2016**, 138, 4608-4615.

10. Fabbro, D.; Cowan-Jacob, S. W.; Moebitz, H., Ten things you should know about protein kinases: IUPHAR Review 14, Brit J Pharmacol **2015**, 172, 2675-2700.

11. Beck, J. R., Lawrence, A., Tung, A. S., Harris, E. N. and Stains, C. I. Interrogating Endogenous Protein Phosphatase Activity with Rationally Designed Chemosensors. ACS Chem Biol **2016**, 11: 284-290.

12. Beck JR, Truong T, Stains CI. "Temporal Analysis of PP2A Phosphatase Activity During Insulin Stimulation Using a Direct Activity Probe." ACS Chem Biol. **2016**, 16;11(12):3284-3288.

13. Shults, M. D.; Imperiali, B., Versatile fluorescence probes of protein kinase activity, J Am Chem Soc **2003**, 125, 14248-14249.

14. Shults, M. D.; Janes, K. A.; Lauffenburger, D. A.; Imperiali, B., A multiplexed homogeneous fluorescence-based assay for protein kinase activity in cell lysates, Nat Methods **2005**, 2, 277-283.

15. Shults, M. D.; Carrico-Moniz, D.; Imperiali, B., Optimal Sox-based fluorescent chemosensor design for serine/threonine protein kinases, Anal Biochem **2006**, 352, 198-207.

16. Lukovic, E.; Gonzalez-Vera, J. A.; Imperiali, B., Recognition-domain focused chemosensors: versatile and efficient reporters of protein kinase activity, J Am Chem Soc **2008**, 130, 12821-12827.

17. Lukovic, E.; Vogel Taylor, E.; Imperiali, B., Monitoring protein kinases in cellular media with highly selective chimeric reporters, Angew Chem Int Ed Engl **2009**, 48, 6828-6831.

18. Stains, C. I.; Tedford, N. C.; Walkup, T. C.; Lukovic, E.; Goguen, B. N.; Griffith, L. G.; Lauffenburger, D. A.; Imperiali, B., Interrogating signaling nodes involved in cellular transformations using kinase activity probes, Chem Biol **2012**, 19, 210-217

19. Stains, C. I.; Lukovic, E.; Imperiali, B., A p38alpha-selective chemosensor for use in unfractionated cell lysates, ACS Chem Biol **2011**, 6, 101-105.

20. Peterson, L. B.; Yaffe, M. B.; Imperiali, B., Selective mitogen activated protein kinase activity sensors through the application of directionally programmable D domain motifs, Biochemistry **2014**, 53, 5771-5778.

21. Beck, J. R.; Peterson, L. B.; Imperiali, B.; Stains, C. I., Quantification of protein kinase enzymatic activity in unfractionated cell lysates using CSox-based sensors, Curr Protoc Chem Biol **2014**, 6, 135-156.

22. Li, M.; Luraghi, P.; Amour, A.; Qian, X. D.; Carter, P. S.; Clark, C. J.; Deakin, A.; Denyer, J.; Hobbs, C. I.; Surby, M.; Patel, V. K.; Schaefer, E. M., Kinetic assay for characterization of spleen tyrosine kinase activity and inhibition with recombinant kinase and crude cell lysates, Anal Biochem **2009**, 384, 56-67.

23. Desai, B.; Dixon, K.; Farrant, E.; Feng, Q.; Gibson, K. R.; van Hoorn, W. P.; Mills, J.; Morgan, T.; Parry, D. M.; Ramjee, M. K.; Selway, C. N.; Tarver, G. J.; Whitlock, G.; Wright, A. G., Rapid discovery of a novel series of Abl kinase inhibitors by application of an integrated microfluidic synthesis and screening platform, J Med Chem **2013**, 56, 3033-3047.

24. Schwartz, P. A., Kuzmic, P., Solowiej, J., Bergqvist, S., Bolanos, B., Almaden, C., Nagata, A., Ryan, K., Feng, J., Dalvie, D., Kath, J. C., Xu, M., Wani, R. and Murray, B. W. Covalent EGFR inhibitor analysis reveals importance of reversible interactions to potency and mechanisms of drug resistance. Proc Natl Acad Sci U S A **2014**, 111: 173-178.

25. Hagel, M., Miduturu, C., Sheets, M., Rubin, N., Weng, W., Stransky, N., Bifulco, N., Kim, J. L., Hodous, B., Brooijmans, N., Shutes, A., Winter, C., Lengauer, C., Kohl, N. E. and Guzi, T. First Selective Small Molecule Inhibitor of FGFR4 for the Treatment of Hepatocellular Carcinomas with an Activated FGFR4 Signaling Pathway. Cancer Discov **2015**, 5: 424-437.

26. Kuzmic, P., Solowiej, J. and Murray, B. W. An algebraic model for the kinetics of covalent enzyme inhibition at low substrate concentrations. Anal Biochem **2015**, 484: 82-90.

27. Cheng H, Nair SK, Murray BW, Almaden C, Bailey S, Baxi S, Behenna D, Cho-Schultz S, Dalvie D, Dinh DM, Edwards MP, Feng JL, Ferre RA, Gajiwala KS, Hemkens MD, Jackson-Fisher A, Jalaie M, Johnson TO, Kania RS, Kephart S, Lafontaine J, Lunney B, Liu KK, Liu Z, Matthews J, Nagata A, Niessen S, Ornelas MA, Orr ST, Pairish M, Planken S, Ren S, Richter D, Ryan K, Sach N, Shen H, Smeal T, Solowiej J, Sutton S, Tran K, Tseng E, Vernier W, Walls M, Wang S, Weinrich SL, Xin S, Xu H, Yin MJ, Zientek M, Zhou R, Kath JC. Discovery of 1-{(3R,4R)-3-[({5-Chloro-2-[(1-methyl-1H-pyrazol-4-yl) amino]-7H-pyrrolo[2,3-d]pyrimidin-4-yl}oxy)methyl]-4-methoxypyrrolidin-1-yl}prop-2-en-1-one (PF-06459988), a Potent, WT Sparing, Irreversible Inhibitor of T790M-Containing EGFR Mutants. J Med Chem. **2016**, 59: 2005-24.

28. Passaro A, Guerini-Rocco E, Pochesci A, Vacirca D, Spitaleri G, Catania CM, Rappa A, Barberis M, de Marinis F. Kennedy SP, Hastings JF, Han JZ, Croucher DR. The Under-Appreciated Promiscuity of the Epidermal Growth Factor Receptor Family. Front Cell Dev Biol. **2016** Aug 22;4:88.

29. Pakkala S Sullivan I, Planchard D. Next-Generation EGFR Tyrosine Kinase Inhibitors for Treating EGFR-Mutant Lung Cancer beyond First Line. Front Med (Lausanne). 2**017** Jan 18;3:76.

30. Kitagawa D1, Yokota K, Gouda M, Narumi Y, Ohmoto H, Nishiwaki E, Akita K, Kirii Y. Activity-based kinase profiling of approved tyrosine kinase inhibitors. Genes Cells **2013**, 18(2):110-22.